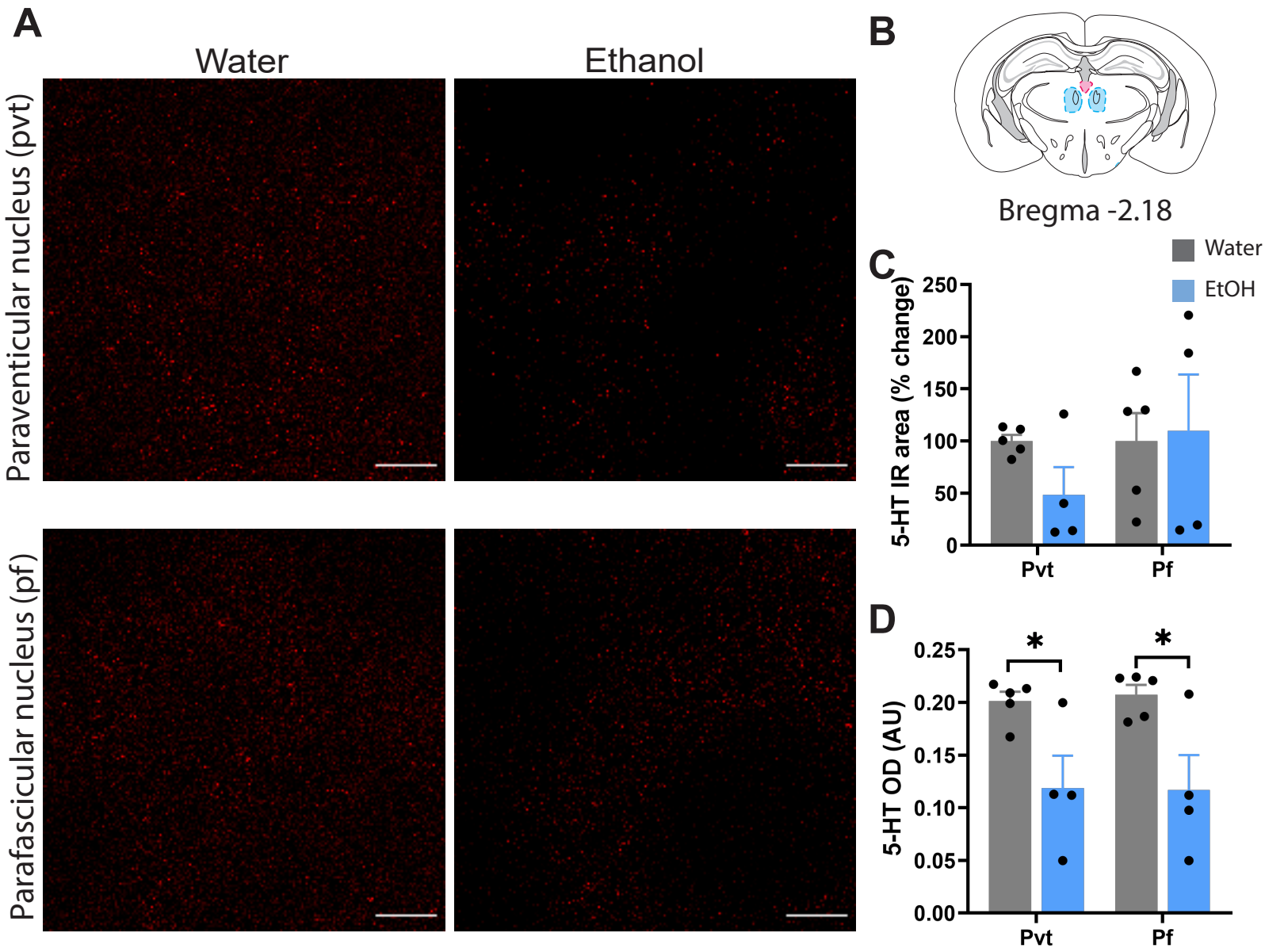

Supplementary Figure 1: Reduced 5-HT expression in the paraventricular and parafascicular nucleus of the thalamus after AIE. (A) Representative confocal images of 5-HT expression in thalamic subregions in water and alcohol drinking mice. (B) Representative regions of interest for the Pvt (blue) and Pf (pink). Histograms of (C) percent change in 5-HT immunoreactive area and (D) optical density in the Pvt and Pf of adult mice following adolescent IA. Scale bar = 50 μm. *p<0.05.

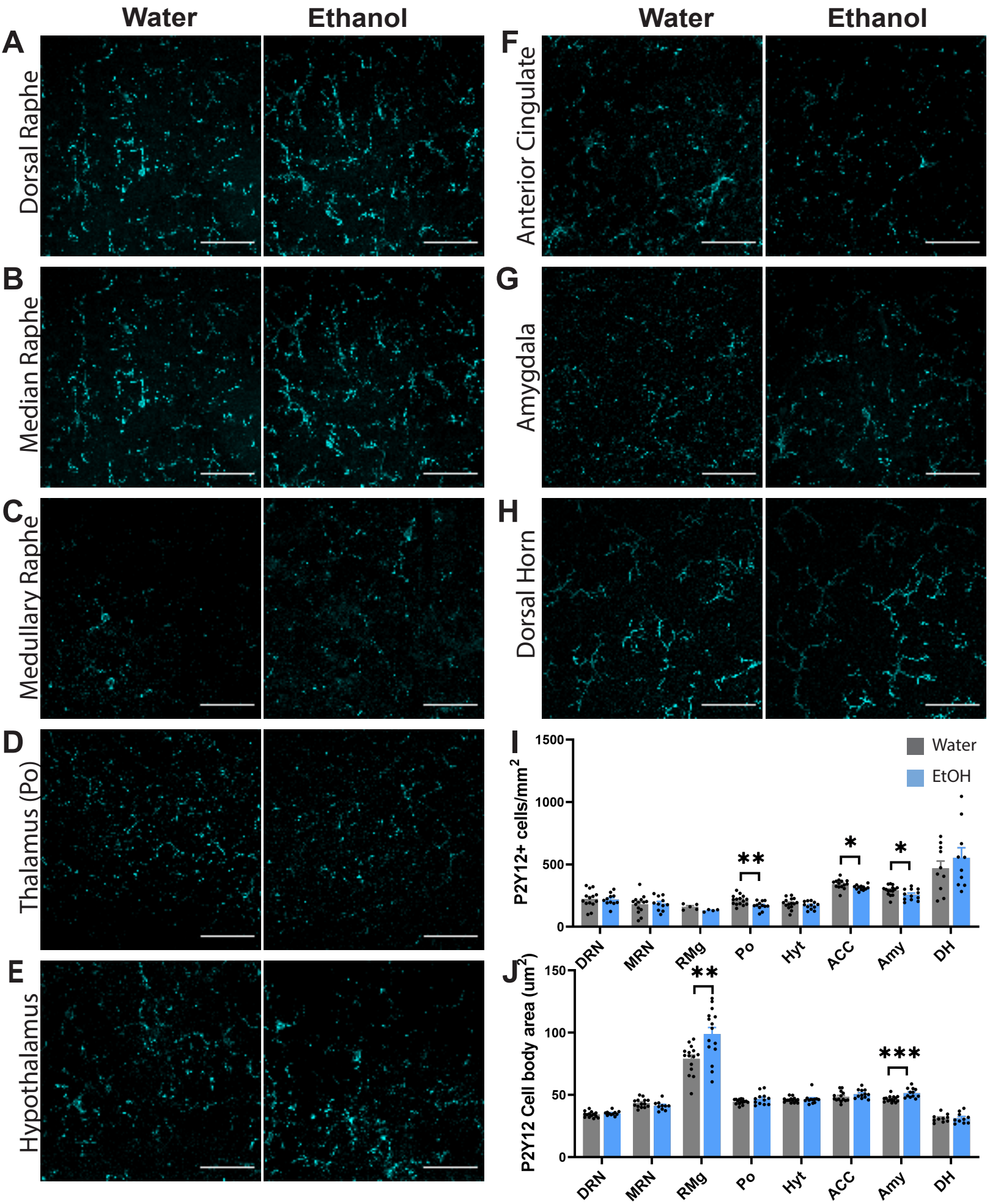

Supplementary Figure 2: Adolescent IA impacts P2Y12 expression in the DRN and downstream regions in adult mice. Representative confocal images of P2Y12+ microglia in the (A) Dorsal raphe nucleus, (B) median raphe nucleus, (C) medullary raphe, (D) posterior complex of the thalamus, (E) hypothalamus, (F) anterior cingulate cortex, (G) amygdala, and (H) dorsal horn. Histograms of (I) P2Y12 cell density and (J) P2Y12 cell body area in the raphe nuclei and downstream regions in adult mice following adolescent IA. Scale bar = 50 μm. *p<0.05, **p<.01, ***p<.001.

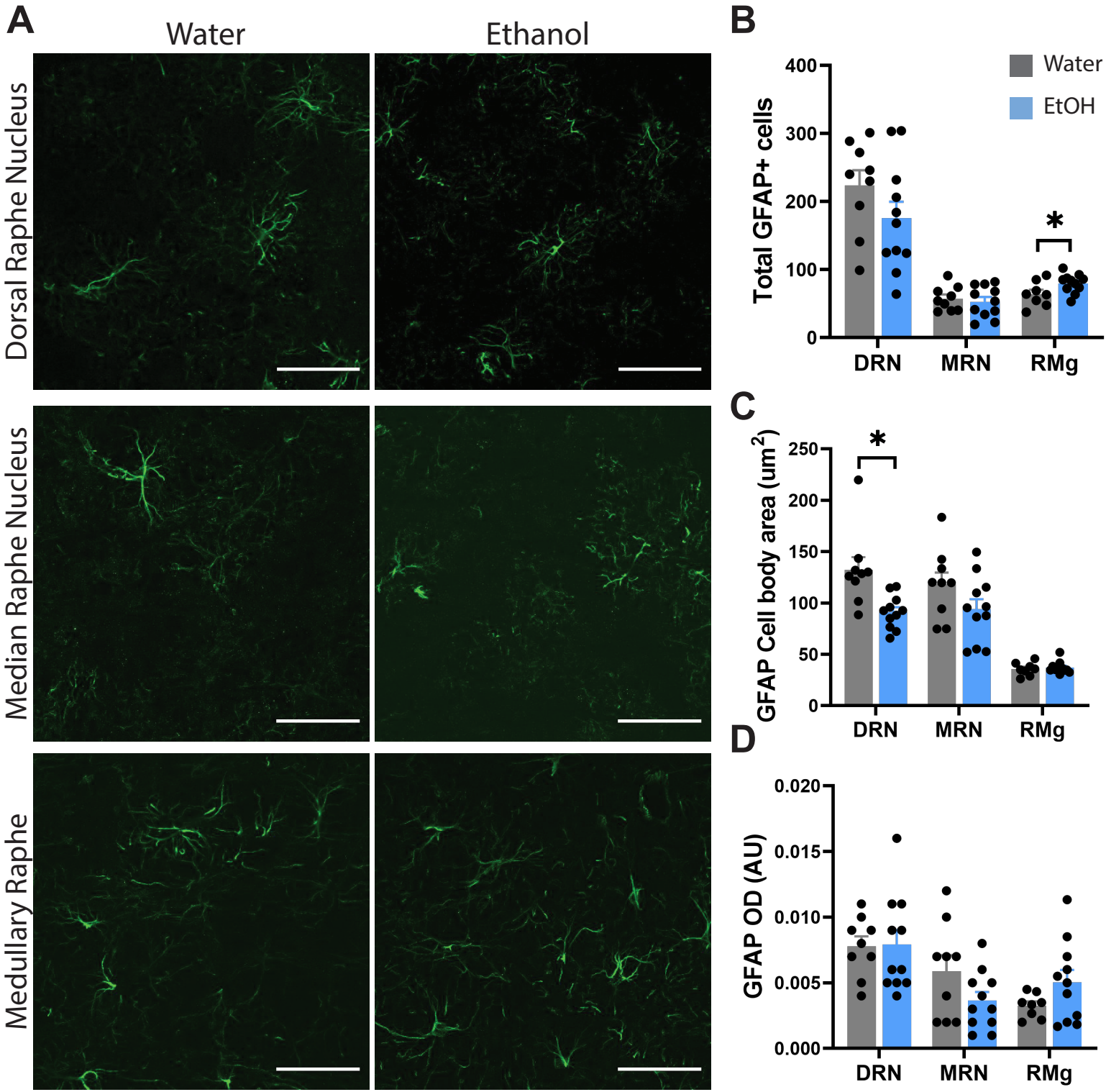

Supplementary Figure 3: Adolescent IA impacts GFAP expression in the raphe nuclei in adult mice. Representative confocal images of GFAP+ astrocytes in the (A) Dorsal raphe nucleus, median raphe nucleus, and medullary raphe. Histograms of (B) GFAP+ cell counts, (C) GFAP cell body area and (D) GFAP optical density in the raphe nuclei in adult mice following adolescent IA. Scale bar = 50 μm. *p<0.05.